MEDDOCS Open Access Publisher

ISSN: 2638-4248

Chronicles of Oncology

Open Access | Research Article

Transcriptomic Profiling Reveals the Novel Role and Mechanism of Interferon-Epsilon (*IFN-Ɛ*) on Human Melanoma

Xuechen Tian[1,2,3,4]*; Zixin Rong[2]; Siew Woh Choo[1,3,4,5]*

[1]Department of Biology, College of Science, Mathematics and Technology, Wenzhou- Kean University, Ouhai, Wenzhou, Zhejiang Province, 325060 China.

[2]Department of Biological Sciences, Xi'an Jiaotong-Liverpool University, Suzhou, China.

[3]Zhejiang Bioinformatics International Science and Technology Cooperation Center, Wenzhou-Kean University, Wenzhou, Zhejiang Province, 325060 China.

[4]Wenzhou Municipal Key Lab for Applied Biomedical and Biopharmaceutical Informatics, Wenzhou-Kean University, Wenzhou, Zhejiang Province, 325060 China.

[5]Dorothy and George Hennings College of Science, Mathematics and Technology, Kean University, 1000 Morris Ave, Union, NJ 07083, USA.

***Corresponding Author(s): Xuechen Tian[1] & Siew Woh Choo[2]**

[1]Wenzhou Municipal Key Lab for Applied Biomedical and Biopharmaceutical Informatics, Wenzhou-Kean University, Wenzhou, Zhejiang Province, 325060 China.

[2]Department of Biology, College of Science, Mathematics and Technology, Wenzhou-Kean University, Ouhai, Wenzhou, Zhejiang Province, 325060 China.

Email: tianxuechen@wku.edu.cn & cwoh@wku.edu.cn

Abstract

Melanoma, known for its aggressive progression and metastatic potential, remains a significant therapeutic challenge. This study aimed to investigate the anti-cancer effects of human *IFN-ε*, a neotype I interferon with potential tumor-inhibiting and immune-modulating properties, on melanoma cells. Utilizing cell viability assays on the melanoma cancer cell line, we found that interferon-epsilon notably inhibits melanoma cell proliferation. Morphological examinations further revealed distinct changes in cell structures post *IFN-ε* treatment. Whole-transcriptome profiling unveiled a significant induction of genes within both type I and II interferon signaling pathways in treated samples, suggesting that *IFN-ε* may bolster immunity-related pathways to combat melanoma cell growth. Collectively, our findings spotlight *IFN-ε*'s promising anti-cancer potential, offering novel insights into its therapeutic application in melanoma management and positioning it as a potential candidate for combinatorial cancer treatments.

Received: Nov 26, 2023

Accepted: Dec 14, 2023

Published Online: Dec 21, 2023

Journal: Chronicles of Oncology

Publisher: MedDocs Publishers LLC

Online edition: http://meddocsonline.org/

Copyright: © Tian X & Choo SW (2023). *This Article is distributed under the terms of Creative Commons Attribution 4.0 International License*

Keywords: Interferon-epsilon; Melanoma; Transcriptome sequencing; Anticancer.

Cite this article: Tian X, Rong Z, Choo SW. Transcriptomic Profiling Reveals the Novel Role and Mechanism of Interferon-Epsilon (*IFN-Ɛ*) on Human Melanoma. Chronicles Oncol. 2023; 6(2): 1013.

Introduction

Melanoma, one of the most prevalent skin cancers, is driven by mutations in melanin genes and can manifest in various parts of the human body, including the skin, eyes, ears, and head and neck. Alarmingly, statistics reveal that every two minutes, an individual is diagnosed with melanoma, and every ten minutes, someone succumbs to the disease [1]. The global incidence of melanoma surpasses 1 per 100,000 annually, with a particularly sharp uptick in lighter-skinned populations [2,3]. Characterized by its aggressive nature, rapid progression, and life-threatening metastasis, melanoma presents a significant challenge [4]. Although early detection can render melanoma highly treatable, metastatic melanoma often resists conventional anti-cancer treatments, with a dismal five-year survival rate under 20% [5]. Interferons (*IFNs*) have emerged as powerful genetic drugs with a plethora of biological activities encompassing antiviral, antitumor, immunomodulatory effects, and suppression of cell proliferation [6,7,8]. Since their introduction to the market in 1989, interferons have gained widespread traction in the treatment of various diseases, owing to their multifaceted biological functions [9]. Notably, *IFNs* can activate numerous bio-signaling pathways in tumor cells, influencing cell proliferation, differentiation, invasion,and innate immunity [10,11,12]. They also modulate mechanisms of apoptosis and can indirectly regulate tumor cell growth by affecting various biological processes linked to tumor progression [13].

Human Interferon-Epsilon (*IFN-ε*) is intriguingly positioned within the *IFN* family. Structurally akin to type I interferons in terms of chromosomal localization, receptor binding type, and signaling pathway, it is tentatively classified as a neotype I interferon [14]. *IFN-ε* is ubiquitously expressed in diverse human tissues, including the brain, lung, small intestine, reproductive tissue, and notably, in coronaryartery smooth muscle cells, microvascular endothelial cells, epithelial cells, and mucosal tissues [6,13]. However, being a relatively recent discovery in the interferon family, the antitumor capabilities, immunomodulatory functions, and receptor signaling pathways of *IFN-ε* remain underexplored.

Given the potential of *IFNs* in modulating immune responses and their demonstrated effects on melanoma, understanding the impact of *IFN-ε* on melanoma could be pivotal. In this study, using the well-characterized melanoma cancer cell line SK-MEL 103, we set out to explore the influence of IFN-ε on melanoma. Preliminary investigations employing cell viability assays indicated anti-cancer properties of *IFN-ε* in melanoma cells. These intriguing findings prompted us to delve deeper into the mechanistic underpinnings of this effect. Through high-throughput RNA sequencing, we aimed to unravel the potential molecular pathways through which *IFN-ε* exerts its effects on melanoma, offering a promising avenue for therapeutic interventions in the future.

Materials and methods

Cell culture

Melanoma cells (SK-MEL 103) were grown in Dulbecco Modified Eagle Medium (DMEM) complete medium (HyClone™) was supplemented with 5% fetal bovine serum (FBS, Gibco™), 1 X penicillin-streptomycin (HyClone™). Cells were cultured in a 37°C incubator containing a 5% CO_2 atmosphere. Cells were harvested when cells reached 80-90% confluence.

Cell viability assay

The recombinant human Interferon-Epsilon (*IFN-ε*) (Catalogue No.9667-ME/CF, R&D) used in this study was reconstituted at 250 µg/mL in sterile water (W4502-1L, Sigma) following the manufacturer's instruction. To perform cell viability assays, the WST-1 cell proliferation and cytotoxicity assay kits (Beyotime, Shanghai) were used according to the approach previously described [15]. In Brief, cells were seeded into a 96-well microplate with a density of 2 $x10^3$ cells per well until well attached. Cells were treated with 800 ng/ml of *IFN-ε* for 24 h, 48 h, 72 h, and 96 h, respectively. The concentration of *IFN-ε* was referred to the manufacturer's instruction and previously reported [16]. After that, 10 µl of WST-1 mixture solution was added to each well and incubated for 4 h at 37°C incubator, and the values of the optical density were measured by a microplate reader (Biotek, US) set at a wavelength of 450 nm. Cell viability was presented as a percentage of the control. All experiments were performed in quintuplicate.

Examination of cell morphology

Cell morphology was evaluated as previously described [17,18]. $1x10^4$ cells were seeded in 35 mm cell culture dishes (Thermofisher) and incubated for 24 hours. Cells were washed twice with PBS (Hyclone™) after discarding the medium. Cells were infiltrated with 1 ml of fresh complete medium and treated with (for treatments) or without (for controls) 800 ng/ml of *IFN-ε* for 48 hours. The morphological changes of the cancer cells were inspected by using a phase contrast inverted microscope (Nikon, Japan) with 200X magnifications.

RNA isolation and integrity analysis

Melanoma cells were selected to harvest total RNAs for RNA sequencing. Cells (6 x 10^4 cells) were cultured in a 60 mm culture dish until well attached. The medium was discarded, and cells were washed twice with PBS (Hyclone™), and 3 ml of fresh complete medium was accurately added to each dish. Then, cells were treated with 800 ng/ml of *IFN-ε* for 48 hours, the same volume of sterile water was used as the control. After that, total RNA of each sample was isolated from cells using TRIzol reagent (Invitrogen, CA). The concentration and purity of the total RNA of each sample were assessed by the spectrophotometer (Nano Drop 2000, Thermo Fisher Scientific Inc.), and total RNA integrity was evaluated using the Agilent 2200 Tape Station system (Agilent Technologies, USA).

Library construction and whole-transcriptome sequencing sequencing technology

RNA library preparation and sequencing were performed using Illumina sequencing technology. The NEB Next Poly (A) mRNA Magnetic Isolation Module was used for isolation of poly (A) mRNA to generate mRNA fragmentation. The Proto Script II reverse transcriptase, first-strand synthesis reaction buffer and random primers were used to synthesize the first-strand cDNA, and the second-strand synthesis enzyme mix was used to synthesize the second-strand cDNA. After purification of the double-strand cDNA using beads, the end prep enzyme mix was used to repair both ends andadd a poly (A) tail in one reaction, then adaptors were added to both ends. After that, each sample was carried out 13 cycles of PCR using the P5 and P7 primers, then the PCR products were cleaned up using beads, validated using an Qsep100 (Bioptic, Taiwan, China), and quantified by Qubit 3.0 Fluorometer (Invitrogen, Carlsbad, CA, USA). Finally, the libraries were loaded on an Illumina Novaseq 6000 instrument

and sequenced using a 2 x 150 bp Paired-End (PE) configuration according to the manufacturer's instructions. Image analysis and base-calling were performed by the Illumina RTA software.

Read preprocessing and mapping

All raw sequences generated by RNA sequencing were obtained in the format of fastq files. Sequences such as adapters and low-quality bases (< Q20) were removed by Cutadapt (V1.9.1) software in order to generate high-quality clean reads [43]. The clean reads were mapped to the human reference genome (GRCh37 download from ENSEMBL) using Hisat2 (v 2.0.1) [19].

Gene expression quantification, normalization and differential expression analyses

For each sample, gene expression levels were estimated using feature count values generated by Subread (v1.6.4) software [20]. The raw counts of all samples obtained by Sub read (v1.6.4) were normalized using DESeq2 (v3.10) [21], in order to make these samples comparable. To examine whether the normalization method works, we constructed and compared the box plots before and after the normalization using R scripts [22]. To identify differentially expressed genes, comparisons were performed between controls (MC) and treated samples (MT) using the well-established DESeq2 Bioconductor package (v.3.10) [21]. Genes were defined as significantly differentially expressed between the two sample groups if the fold change ≥2 or 1.5 and False Discovery Rate (FDR) < 0.05. Differential expression genes with positive logarithmic Fold Change (FC ≥ 2 or 1.5) levels in MT (melanoma treatment group) compared with MC (melanoma control group) were defined as "up-regulated", otherwise, the negative logarithmic fold change (FC ≤ −2 or −1.5) levels were expressed as "down-regulated".

GO annotation and enrichment analysis

Gene Ontology (GO) analysis was performed on significant differentially expressed genes in melanoma cells based on the PANTHER classification system on the Gene Ontology website (http://geneontology.org) [23,24]. All significant differentially expressed genes were mapped to each GO term of the PANTHER classification system to calculate the number of genes enriched corresponding to each GO term and pathway term. Fisher's exact test and calculate FDR were conducted in analysis and only results selected for FDR P< 0.05. The final annotation result categorized with respect to Biological Process, Molecular Function, as well as Reactome pathway.

Statistical analysis

Statistical results of cell viability assay were expressed as mean ± SEM based on five independent biological replicates. The differences between the treatment groups and control were operated by unpaired *t*-test and were considered statistically significant at $P < 0.05$. Statistical analysis of cell viability was performed using Graph Pad Prism 7 [25].

Results

***IFN-ε* can inhibit the proliferation of melanoma cells**

The WST-1 cell proliferation and cytotoxicity assay was selected to evaluate the cell viabilities of *IFN-ε* on melanoma cells based on the method previously reported [15]. Cells were treated with 800 ng/ml of *IFN-ε* for 24 h, 48 h, 72 h, and 96 h separately. Our data suggested that *IFN-ε* showed significant inhibition effects on the viability of melanoma cells compared with the control group at 48 h with the reduction of approximately 10% of cell viability (P< 0.0001) at 48 h after the treatment (**Figure 1a**). Results suggested that *IFN-ε* can in hibit the proliferation of melanoma cells, with the best effects at 48 h after the treatments.

Effects of *IFN-ε* on the morphological changes of melanoma cells

To investigate the reason that could affect cell proliferation, we performed the morphological changes examination of cancer cells according to the method previously reported by [18]. After treatment with *IFN-ε* for 48 h, we examined the morphology of melanoma cells. Interestingly, we observed distinct morphological changes in the melanoma cells compared with the control group (**Figure 1b-c**). The visualized results of the control (untreated) cells showed that cells grew and attached well. Meantime, cells remained in their original form, and only a few cells showed nuclear contraction. In contrast, cells treated with *IFN-ε* (800 ng/ml) showed a significant reduction in the number of cells in the same field of view, and the cell morphology exposure to typical aberrant features such as nuclear fragmentation, apoptotic bodies, bubbling and echinoid spikes, especially the apoptotic bodies were in a high frequency. Our results suggested that *IFN-ε* can affect the morphology of some melanoma cells, probably causing the death of these cancer cells.

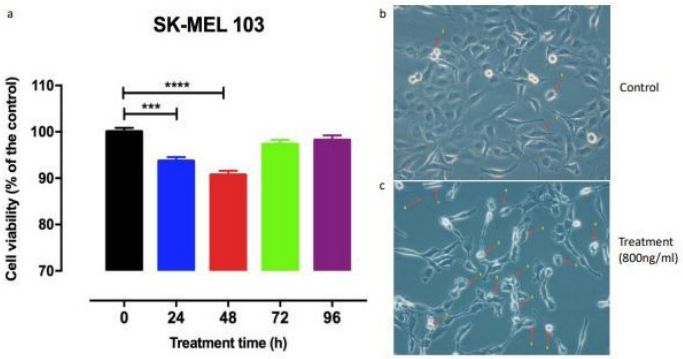

Figure 1: Cell viability assay and examination of cell morphology.

(a) *IFN-ε* inhibits cancer cell proliferation in a time-dependent manner; the viabilities of melanoma cells at different treatment times were measured by WST-1 assay, and the concentration of *IFN-ε* was 800 ng/ml (n=5 plates, 3 well replicates per plate). *P<0.05, **P<0.01, ***P<0.0005, ****P<0.0001. (b-c) Selected representative photomicrographs showed morphological changes in melanoma cells. Cells were imaged by an inverted phase contrast microscope set at magnification 200X after being treated with 800 ng/ml of *IFN-ε* for 48 hours. Marks indicate (1) normal cell, (2) condensed nuclei, (3) cell shrinkage, (4) membrane blebbing, (5) apoptotic bodies, (6)nuclear fragmentation, (7) bubbling, (8) echinoid spikes.

RNA isolation and quality assessment

To further explore the underlying mechanism of *IFN-ε* on human melanoma cancer, we performed whole-transcriptome sequencing by comparing the control (untreated) with the *IFN-ε* treated samples (treatment). Three biological replicates were used for each group. The quality/integrity of the extracted total RNAs of samples were evaluated using the Agilent 2200 Tape Station system. The integrity of all RNA samples was high (RIN=10), indicating the high quality of our RNAs for high-throughput sequencing (**Figure 2 and Table S1**).

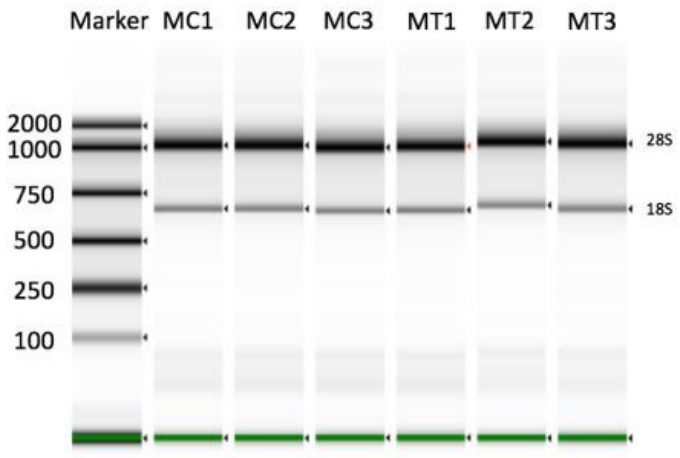

Figure 2: Gel image of RNA integrity assessment by Agilent 2200 Tape Station system.

MC: Melanoma Cell Control Group, MT: Melanoma Cell Treatment Group, the 28S and 18S bands were bright, and the brightness of 28S was more than twice that of the 18S, which means that the RNA quality was perfect. Meanwhile, the concentration and purity of the total RNA of each sample were assessed by the spectrophotometer and Agilent 2200 Tape Station system. The ratio of absorption at 260 nm / 280 nm was above 1.9. The RNA Integrity Number (RIN) of all samples was 10, and the RNA quality level was A (**Table S1**).

Whole-transcriptome sequencing and analysis

All RNA was used for library construction and RNA sequencing, and raw sequence data generated by the Illumina instrument (Novaseq 6000) was performed for quality control. All raw data that passed the quality assessment were used for transcriptome analysis. Actually, a total of 227.2 million paired-end raw reads of 150 bp read length were generated from six samples (**Table S2**). After the removal of low-quality reads, a total of 276.3 million paired-end clean reads of 150 bpread length were shown in **Table 1**. The overall Q30 percentage was above 90%, and N content was lower than 3.09, which indicates that data preprocessing was successful for alignment.

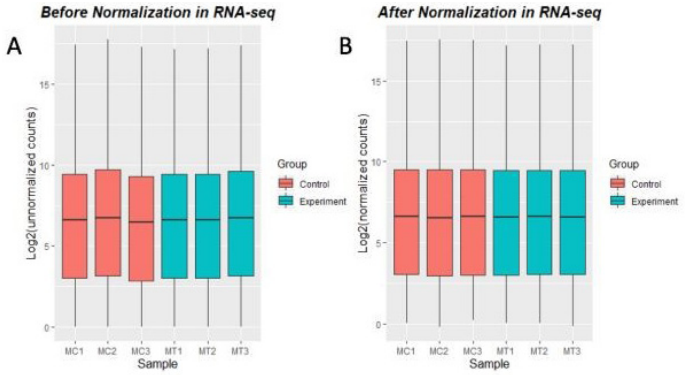

Figure 3: Box plots for normalization. Distribution of read counts in RNA-seq, the ordinate indicates log2 (normalized or unnormalized counts), the x-axis indicates the sample name of each group, control group: (MC1, MC2, MC3) and treatment group: (MT1, MT2, MT3). (A) Distribution of the unnormalized read counts. (B) Distribution of the unnormalized read counts.

Table 1: The clean data of each sample was counted after filtering low-quality data.

Samples	Avg Read Length (bp)	Number of Reads	Bases	Q20(%)	Q30(%)	GC(%)	N (ppm)
MC1	148.63	44650030	6636497923	97.36	92.76	48.95	2.87
MC2	148.53	53267710	7912078090	96.48	90.91	48.07	2.73
MC3	148.58	39896884	5927686979	97.04	92.10	48.14	2.93
MT1	148.89	44223910	6584323645	96.75	91.50	48.45	2.85
MT2	148.67	44486072	6613588502	96.79	91.63	48.92	2.93
MT3	148.66	49861882	7412658589	97.01	92.08	49.00	2.95

After mapping to the hg37 reference genome using Hisat2, we performed an alignment quality assessment. More than 89% of total reads of paired-end were mapped to reference genes in all 6 samples, and unique-mapping reads account for 84% above (**Table S3**). These results illustrate a good quality of clean reads and of the reads alignment.

Transcript abundance assessment and differential expression analysis of melanoma cells

Before comparing the expression profiles of the two groups of samples, we normalized all samples (**Figure 3**). The normalized data indicates that the normalization of six samples worked well and the data was suitable for comparison and differential expression analysis. After comparison of the expression profiles between the control (MC) and treatment (MT) groups, we successfully identified 34 differentially expressed genes consisting of 31 up-reguleated genes and 3 down-reguleated genes when the cut off of fold changes of 2 and FDR/Padj <0.05 were used (**Table 2 and Figure 4A**). As shown in **Table 2(as well as Figure 4B)**, while the more relaxed cut off (fold change ≥ 1.5) was used, we can identified 68 significant differentially expressed genes including 54 up-regulated genes and 14 down-reguleated genes. By manually examining the two sets of genes from the two used cut offs, we found they are generally very similar. Therefore, we decided to use the genes set from the more stringent cut off (fold change ≥ 2) for downstream analyses.

Table 2: Number of differential expression genes in melanoma cells.

Control-VS-treatment	Up	Down	Fold change (Cutoff)
MC-VS-MT	31	3	2
MC-VS-MT	54	14	1.5

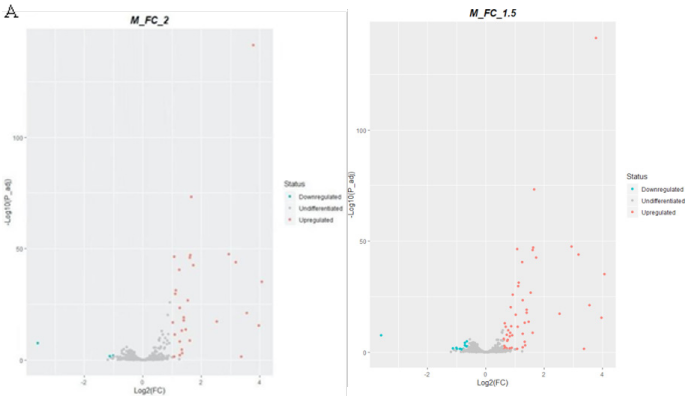

Figure 4: Volcano plots of differentially expression genes.

The red dot represents the up-regulated genes, and the blue dots represent the down-regulated genes. The abscissa indicates the log 2 (fold change) value, and the ordinate represents the mean expression value of log10 (Padj).

Interestingly, among the 31 up-regulated genes in the *IFN-ε* treated melanoma cells, we found many interferon-induced protein family members including OAS2, IFI44L, IFI6, IFIT1, IFI27, IRF9, IFIT3, IFI44 and the innate immunity-related protein members such as ISG15, PARP9 and IRF7, were also significantly induced (**Table 3**). Among the interferon-induced proteins, the OAS2 and IFI44L showed significant induction with approximate 16-fold changes. The OAS2 protein is the dsRNA-activated antiviral enzyme that can mediate the antiviral effects via the activation of RNASEL to cause the degradation of cellular viral RNA to inhibit protein synthesis and terminate viral replication [26]. Besides, it has been reported to play a critical role in cellular processes such as proliferation, differentiation, apoptosis and gene regulation [27].The potent induction of OAS2 might reveal a potential function of *IFN-ε* in suppressing cancer cell proliferation.

We cannot rule out the possibility that some real differentially expressed genes may have been regulated with very low fold change (e.g. < 2). Therefore, we wondered whether the outcome/GO enrichment would be the same if we used the list of the genes generated from the fold change ≥1.5 (gene list 1.5, **Table S4**). As anticipated, although we managed to slightly increase the number of genes, but the enriched GO terms are generally similar or consistent to the results for the genes list from the fold change ≥ 2. For example, most of these genes were enriched in the innate immunity-related processes (**Figure S1**). Therefore, we decided to stick to the list of the genes generated from the stringent cutoff of the fold change of ≥ 2.

Table 3: Summary of differential expression genes with the cutoff of fold change ≥ 2.

Gene ID	Fold Change	Gene symbol	MC vs. MT	Gene description
ENSG00000111335	16.73	OAS2	up	2'-5'-oligoadenylate synthase 2 OAS2
ENSG00000137959	15.62	IFI44L	up	Interferon-induced protein 44-like IFI44L
ENSG00000126709	13.61	IFI6	up	Interferon alpha-inducible protein 6 IFI6
ENSG00000185745	11.69	IFIT1	up	Interferon-induced protein with tetratricopeptide repeats 1 IFIT1
ENSG00000204375	10.24	XAGE1E	up	X antigen family, member 1E
ENSG00000165949	8.98	IFI27	up	Interferon alpha-inducible protein 27, mitochondrial IFI27
ENSG00000089127	7.67	OAS1	up	2'-5'-oligoadenylate synthase 1 OAS1
ENSG00000133106	5.77	EPSTI1	up	Epithelial-stromal interaction protein 1 EPSTI1
ENSG00000187608	3.31	ISG15	up	Ubiquitin-like protein ISG15 ISG15
ENSG00000130589	3.15	HELZ2	up	Helicase with zinc finger domain 2HELZ2
ENSG00000111331	3.06	OAS3	up	2'-5'-oligoadenylate synthase 3 OAS3
ENSG00000138496	3.03	PARP9	up	Poly [ADP-ribose] polymerase 9 PARP9
ENSG00000184979	3.02	USP18	up	Ubl carboxyl-terminal hydrolase 18 USP18
ENSG00000138642	2.91	HERC6	up	Probable E3 ubiquitin-protein ligase HERC6 HERC6
ENSG00000137628	2.77	DDX60	up	Probable ATP-dependent RNA helicase DDX60 DDX60
ENSG00000115267	2.63	IFIH1	up	Interferon-induced helicase C domain-containing protein 1 IFIH1
ENSG00000177409	2.63	SAMD9L	up	Sterile alpha motif domain-containing protein 9-like SAMD9L
ENSG00000134326	2.53	CMPK2	up	UMP-CMP kinase 2, mitochondrial CMPK2
ENSG00000100918	2.50	REC8	up	Meiotic recombination protein REC8 homolog REC8
ENSG00000108771	2.50	DHX58	up	Probable ATP-dependent RNA helicase DHX58 DHX58
ENSG00000213928	2.41	IRF9	up	Interferon regulatory factor 9 IRF9
ENSG00000119917	2.38	IFIT3	up	Interferon-induced protein with tetratricopeptiderepeats 3 IFIT3
ENSG00000259529	2.38	RP11-468E2.4	up	E3 ubiquitin-protein ligase RNF31
ENSG00000137965	2.36	IFI44	up	Interferon-induced protein 44 IFI44
ENSG00000101347	2.19	SAMHD1	up	Deoxynucleoside triphosphate triphosphohydrolase SAMHD1 SAMHD1
ENSG00000173193	2.14	PARP14	up	Poly [ADP-ribose] polymerase 14 PARP14
ENSG00000059378	2.12	PARP12	up	Poly [ADP-ribose] polymerase 12 PARP12

ENSG00000185507	2.11	IRF7	up	Interferon regulatory factor 7 IRF7
ENSG00000115415	2.11	STAT1	up	Signal transducer and activator of transcription 1-alpha/beta STAT1
ENSG00000188313	2.04	PLSCR1	up	Phospholipid scramblase 1 PLSCR1
ENSG00000251196	2.01	RP11-54F2.1	up	Uncharacterized protein (Fragment) unassigned
ENSG00000218175	-2.01	AC016739.2	down	Uncharacterized protein (Fragment) unassigned
ENSG00000234009	-2.20	RPL5P34	down	ribosomal protein L5 pseudogene 34
ENSG00000237550	-11.98	UBE2Q2P6	down	ubiquitin-conjugating enzyme E2Q family member 2 pseudogene 6

Functional enrichment analysis.

To better understand the functions of the differentially expressed genes, we performed the functional enrichment analysis using the PANTHER classification system on the Gene Ontology (GO) website [23,24]. Our results showed that the GO molecular function and GO biological progress were significantly enriched in melanoma samples treated by *IFN-ε* compared with the control sample (**Figure 5**). For biological processes, the highest term was related tothe type I interferon signaling pathway, with 41% of genes assigned. These terms, including viral process, interferon-gamma-mediated signaling pathway, and negative regulation of viral genome replication, were also significantly enriched, accounting for 24%, 21%, and 17%, respectively. In addition, there was 10% of genes assigned to the innate immune response and others to the type I or type II signaling pathway **(Figure 5)**. The first five top terms were mostly associated with the innate antiviral response, and other cellular processes such as proliferation, differentiation, and gene regulation, which proved that they are involved in a wide range of mechanisms that mediates the host immune responses in tumor [7]. In particular, most of the genes associated with the type I signaling pathway such as OAS2, ISG15, STAT1, IFI6, IRF9, etc. were involved in the mechanism that mediate immuneresponse in cancer [7,28,29]. These results suggest that *IFN-ε* has an effect on melanoma cells by inducing innate immunity, such as the type I and type II interferon signaling pathways. For molecular function, the DEGs were mainly assigned to binding and enzyme activity (**Figure 5**). The top represented binding terms were carbohydrate derivative binding, nucleotide binding, purine ribonucleoside triphosphate binding, and double-stranded RNA binding, accounting for 38%, 38%, 34%, and 21%, respectively. Top represented activity terms including RNA helicase activity, NAD+ADP-ribosyl transferase activity and 2'-5'-oligoadenylate synthetase activity were mapped to 14%, 10% and 10%, individually.

To further identify the pathway in which the DEGs are involved, DEGs were analyzed by the PANTHER classification system (GENEONTOLY) and Reactome pathway annotation [24]. Our analysis showed that the differentially expressed genes (41%) were mostly enriched in the interferon-alpha/beta signaling, followed the type II signaling, the DDX85/IFIH1-mediated induction of interferon- alpha/beta, and ISG15 antiviral mechanisms (**Figure 6**). Interestingly, it has been reported that the activated interferon signaling can play an important anti-cancer role by activating the JAK-STAT pathway, which activates the immune response [30]. Therefore, the pathway analysis indicates that *IFN-ε* may kill cancer cells by activating the interferon signaling pathway to regulate the immune response.

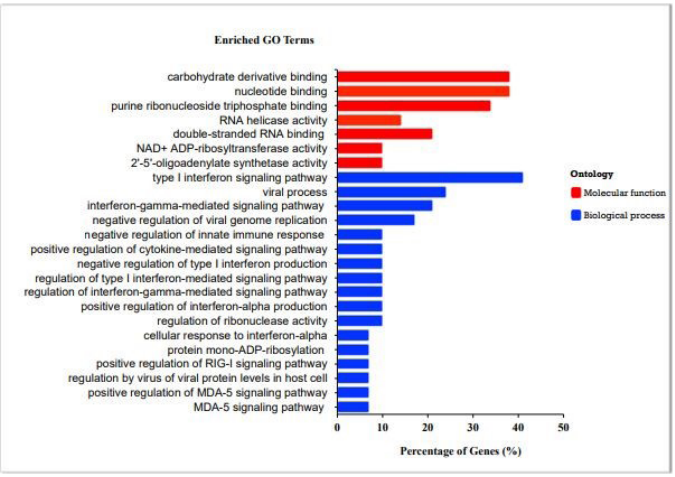

Figure 5: Functional enrichment analysis.

Red bars are the enriched molecular function terms (p< 0.05), whereas the blue bars are the enriched biological processes.

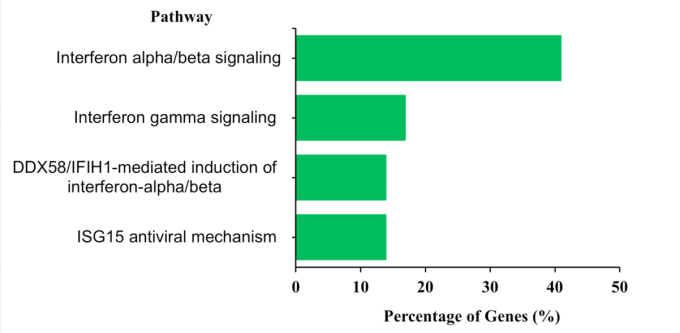

Figure 6: The enrichment analysis of the reactome pathways.

Discussion & conclusion

Here we have first time studied the effect of the *IFN-ε* on the aggressive melanoma cells. Our cell viability assays clearly showed that the *IFN-ε* has effects on the melanoma cell line, as well as alters its cell morphology, such as condensed nuclei, cell shrinkage, and nuclear fragmentation, although the reduction of the melanoma cells was about 10% after the *IFN-ε* treatment. However, we believe that the change is authentic as supported by the observations of the changes in cell morphology. Besides that, our whole-transcriptome analysis has also revealed that many innate immunity-related pathways are significantly upregulated after the treatment with *IFN- ε*. These pathways are relevant and known to be able to kill cancer cells in many previous studies [31,32,7,8].

In the morphological examination, we observed some morphological changes such as condensed nuclei, cell shrinkage, membrane blebbing, apoptotic bodies, nuclear fragmentation, bubbling and echinoid spikes in melanoma cells after the treatment with *IFN-ε*. Although these similar morphological features have been defined as the main features of apoptosis in previously reported [17,18,33], however we could not conclude whether these morphological changes were caused by apoptosis until we perform apoptotic assays in the future. We cannot rule out the possibility that these morphological changes could be due to other mechanisms caused by *IFN-ε*. For instance, in 1990, Glaus and colleagues defined this morphological change induced by type I and type II interferon on melanoma cells as immunophenotypic changes, which were attributed to three different mechanisms: (1) the induction of terminal differentiation of transformed cells, (2) a direct anti-proliferative effect, and (3) a modulation of cell surface antigens on the tumor cell with activation of the host's immune system [32]. Since our RNA-Seq analysis showed that *IFN-ε* can activate the type I and type II interferon pathways, we believe that the changes in the cell morphology of melanoma cells are likely immunophenotypic changes. However, additional experiments need to be performed in order to validate whether these morphological changes are due to apoptosis or immunophenotypic in the future by the evaluation method previously reported [32].

For differential expression gene analysis, with the up-regulation of interferon-induced protein family member and immune-related protein in melanoma cells treated by *IFN-ε*, this exposed to that *IFN-ε* was involved in related mechanisms that regulate immune response in melanoma cells, and balancing between immune escape and immune surveillance. Among these up-regulated genes such as OAS1, STAT1, IFI6, IRF7, IRF9, IFI27 and ISG15, were associated to the type I interferon signaling pathway in previous study [34,35,36], the finding was consistent with our analysis of the biological process (**Figure *5***). Type I interferon signaling leading to transcription of Interferon-Stimulated Genes (ISGs) by activating the Janus Kinase (JAK) pathway and phosphorylation of transcription (STAT) pathway [37]. Furthermore, our data also revealed that some up-regulated genes, including OAS, STAT1, IRF7, and IRF9, were enriched in the interferon-gamma-mediated signaling pathway and the interferon-gamma signaling. The interferon-gamma signaling has been reported to induce tumor ischemia and homeostasis program, resulting in tumor clearance [31]. Therefore, these results suggest that *IFN-ε* led to the upregulation of interferon-gamma signaling and in turn clearance of tumor cells, which was consistent to the immune checkpoint blockade reported in recent years that can up-regulate interferon-gamma signaling to clear cancer [39,39]. And this reveals that *IFN-ε* may be a ponderable candidate for cancer immunotherapy.

Furthermore, interferons have a dual role as either cancer promoters or suppressors in various tumor types and microenvironments, and they are involved in many biological processes cascade such as cellular immune response against viral/bacterial infections to proliferation and apoptosis [7]. Once the interferon type I genes are knocked out and down-regulation of their receptors of signaling molecules such as STAT1 and IFR9 involved in the interferon signaling pathway, cancer cells ignore all regulatory functions and effects that target them [7]. These findings indicate that all genes such as STAT1, IFR9, IFI27, IRF7 and ISG15 from the interferon type I signaling cascade play a crucial role in suppressing and clearing of cancer cells. Interestingly, in our study, these genes were significantly up-regulated in melanoma cells after we treated the cells with interferon- ε, supporting our view that *IFN-ε* may activate the type I interferon signaling pathway to suppress the cell proliferation and survival of melanoma cells. In the meantime, we also found that some genes such as DXH58 and IFIT were enriched in a negative regulation of type I interferon production, probably implying that *IFN-ε* may be a potential mechanism that, in turn helps cancer cells escape by negative regulation of type I production. It has been proven that cancer cells often abrogate interferon production to successfully metastasize shown by Greiner and his colleagues in 1984 [40].This may partially explain why *IFN-ε* only showed a 10% inhibition efficiency in our cell viability assay.

Our RNA-Seq data showed that many interferon-related genes were induced in the *IFN-ε* treated melanoma cells. They may indirectly regulate cancer cell proliferation, affecting various biological processes including angiogenesis and immune response, involved in tumor progression. As previously emphasized by Gresser and and colleagues, inter ferons can increase survival in mice affected by lymphocytic leukemia regardless of the sensitivity of tumor cells to the interferon drugs [41]. In fact, interferon serves as an activator in several immune cells such as macrophages, T cells, B cells and NK [7]. This fully exposes the indirect relationship between *IFN-ε* and tumor immunity. Simultaneously, the activation of the JAK / STAT signaling cascade is achieved by triggering phosphorylation of Tyr2 and Jak1 through the binding of type I interferons to its receptors IFNAR1 and IFNAR2 [37]. In melanoma, STAT plays an important role in mediating the transcription of tumor suppressor promyelocytic leukemia proteins, which inhibits the proliferation of malignant melanoma-initiating cells [7]. Therefore, we speculate that *IFN-ε* may also activate the phosphorylation of tyrosine and JAK by binding to the receptors on the cell surface, thereby activating the JAK / STAT signaling pathway.

Our cell viability assays showed *IFN-ε* has only a 10% inhibition efficiency in melanoma cells. Perhaps, the low inhibitory effect could be explained by several possibilities. Firstly, the tumor cells have a complex microenvironment, with various receptors attached to the cell surface, and each tumor cell also has individual differences [42]. *IFN-ε* may achieve the anti-cancer effect by binding to the receptors on the cancer cell surface. However, it is possible that not all cancer cells have the receptor bound by *IFN-ε*. Therefore, *IFN-ε* may only kill some of these cancer cells. Secondly, our data suggest that *IFN-ε* could be good as a candidate for immunotherapy since our data showed that it could activate innate immunity-related pathways in the cancer cells. Many immunotherapies usually use a combination of drugs in order to achieve good efficacy. Therefore, we believe that the efficacy of *IFN-ε* should be enhanced if we combine it with other drugs in treating cancers.

In conclusion, we have successfully shown that *IFN-ε* has anti-cancer effect on human melanoma. We have also shown that it may kill the cancer cells likely by activating the innate immunity-related pathways, providing a possible novel candidate for immunotherapy in aggressive melanoma cancer. However, more laboratory work needs to be done in order to further evaluate its efficacy in anti-cancer in the future.

Supplemental information

Supplemental information contains **Figure S1 and Table S1-4,** and sequencing data is available online with an accession number: PRJNA1047146.

Author contributions

S.W.C. and X.T. conceived this project and wrote the manuscript. ZR, and XT. collected the data, analyzed the data, and made the figures. S.W.C. supervised and managed the project and acquired the funding. X.T. and S.W.C conducted the data interpretation and revised the manuscript. All authors prepared, read, and approved the final version of the manuscript.

Funding

This work was funded by the high-level talent recruitment programme for academic and research platform construction (Reference Number: 5000105) from Wenzhou- Kean University.

Acknowledgments

We would like to thank Dr. Ferdinand Kappes of Biology Department of Xi'an JiaotongLiverpool University for providing the melanoma cell lines used in this study. We acknowledge that most of the work was supported by the Biology Department of Xi'an Jiaotong Liverpool University.

Conflict of interest statement

The authors declare that the research was conducted without any commercial or financial relationships that could be construed as a potential conflict of interest.

References

1. Siegel Rl, Miller KD, Fuchs HE, Jemal A, et al. Cancer Statistics, Cancer J Clin. 2021; 71: 7-33.

2. Ernst M, Giubellino A. The Current State of Treatment and Future Directions in Cutaneous Malignant Melanoma. Biomedicines. 2022; 10.

3. Tufail M, Wu C. Cancer Statistics in Pakistan From 1994 to 2021: Data from Cancer Registry. JCO Clin Cancer Inform. 2023; 7: E2200142.

4. Miller AJ, Mihm MC, JR. Melanoma. N Engl J Med. 2006; 355: 51-65.

5. Dong L, Tian X, Zhao Y, Tu H, Wong A, et al. 2022. The Roles of MiRNAs (MicroRNAs) in Melanoma Immunotherapy. Int J Mol Sci. 2022; 23.

6. Peng FW, Duan ZJ, Zheng LS, Xie ZP, Gao HC, et al. Purification of recombinant human interferon-epsilon and oligonucleotide microarray analysis of interferon-epsilon-regulated genes. Protein Expr Purif. 2007; 53: 356-362.

7. Di Franco S, Turdo A, Todaro M, Stassi G, et al. Role of Type I and II Interferons in Colorectal Cancer and Melanoma. Front Immunol. 2017; 8: 878.

8. Dunn GP, Koebel CM, Schreiber RD. Interferons, immunity and cancer immunoediting. Nat Rev Immunol. 2006; 6: 836-848.

9. Gorgulho CM, Romagnoli GG, Kaneno R. Type I Interferons: History and Perspectives as Immunotherapeutic Agents Against Cancer. In: REZAEI, N. (ed.) Cancer Immunology: Bench to Bedside Immunotherapy of Cancers. Cham: Springer International Publishing. 2021.

10. Gorgulho CM, Romagnoli GG, Kaneno R. Type I Interferons: History and Perspectives as Immunotherapeutic Agents Against Cancer. In: REZAEI, N. (ed.) Cancer Immunology: Bench to Bedside Immunotherapy of Cancers. Cham: Springer International Publishing. 2021.

11. LI SF, Gong MJ, Zhao FR, Shao JJ, Xie YL, et al. Type I Interferons: Distinct Biological Activities and Current Applications for Viral Infection. Cell Physiol Biochem. 2018; 51: 2377-2396.

12. Xi Y, Day SL, Jackson RJ, Ranasinghe C. Role of novel type I interferon epsilon in viral infection and mucosal immunity. Mucosal Immunol. 2012; 5: 610-622.

13. De Weerd NA, Samarajiwa SA, Hertzog PJ. Type I interferonreceptors: Biochemistry and biological functions. J Biol Chem. 2007; 282: 20053-20057.

14. Garbe C, Krasagakis K, Zouboulis Cc, Schröder K, Krüger S, et al. Antitumor activities of interferon alpha, beta, and gamma and their combinations on human melanoma cells in vitro: changes of proliferation, melanin synthesis, and immunophenotype. J Invest Dermatol. 1990; 95: 231s-237s.

15. Shi K, Wang X, Zhu J, Cao G, Zhang K, Su Z, et al. Salidroside protects retinal endothelial cells against hydrogen peroxide-induced injury via modulating oxidative status and apoptosis. Biosci Biotechnol Biochem. 2015; 79: 1406-1413.

16. Choo SW, Tian X. A Combination Drug of Human Interferon-ε and Interferon-γ. Australian patent application 2021102398. 2021.

17. Moongkarndi P, Kosem N, Kaslungka S, Luanratana O, Pongpan N, et al. 2004; Antiproliferation, antioxidation and induction of apoptosis by Garcinia mangostana (mangosteen) on SKBR3 human breast cancer cell line. Journal of Ethnopharmacology. 2004; 90: 161-166.

18. Rahman SNSA, Wahab NA, Abd Malek SN. In Vitro Morphological Assessment of Apoptosis Induced by Antiproliferative Constituents from the Rhizomes of Curcumazedoaria. Evidence-Based Complementary and Alternative Medicine. 2013.

19. Kim D, Paggi Jm, Park C, Bennett C, Salzberg SL. Graph-based genome alignment and genotyping with HISAT2 and HISAT-genotype. Nature Biotechnology. 2019; 37; 907-+.

20. Liao Y, Smyth GK, Shi W. The R package Rsubread is easier, faster, cheaper and better for alignment and quantification of RNA sequencing reads. Nucleic Acids Research. 2019; 47.

21. Love MI, Huber W, Anders S. Moderated estimation of fold change and dispersion for RNA-seq data with DESeq2. Genome Biol. 2014; 15: 550.

22. Verzani J. A peer-reviewed, open-access publication of the R Foundation for Statistical Computing Editorial. R Journal. 2018; 10: 4-5.

23. Mi H, Muruganujan A, Casagrande JT, Thomas PD. Large - scale gene function analysis with the PANTHER classification system. Nat Protoc. 2013; 8: 1551-1566.

24. Mi H, Muruganujan A, Huang X, Ebert D, Mills C, et al. Protocol Update for large-scale genome and gene function analysis with the PANTHER classification system (v.14.0). Nat Protoc. 2019; 14: 703-721.

25. Mitteer DR, Greer BD, Fisher WW, Cohrs VL. Teaching Behavior Technicians to Create Publication-Quality, Single-Case Design Graphs in Graphpad Prism 7. Journal of Applied Behavior Analysis. 2018; 51: 998- 1010.

26. Sarkar SN, Ghosh A, Wang HW, Sung SS, Sen GC, et al.1999. Thenature of the catalytic domain of 2'-5'-oligoadenylate synthetases. J Biol Chem. 1999; 274: 25535-25542.

27. Kristiansen H, Gad HH, Eskildsen-Larsen S, Despres P, Hartmann R, et al. The oligoadenylate synthetase family: an ancient protein family with multiple antiviral activities. J Interferon Cytokine Res. 2011; 31: 41- 47.

28. Devries TA, Kalkofen RL, Matassa AA, Reyland ME, et al. Protein kinase Cdelta regulates apoptosis via activation of STAT1. J Biol Chem. 2004; 279: 45603-45612.

29. Takeuchi T, Yokosawa H. ISG15 modification of Ubc13 suppresses its ubiquitin-conjugating activity. Biochem Biophys Res Commun. 2005; 336: 9-13.

30. Parker BS, Rautela J, Hertzog PJ. Antitumour actions of interferons: Implications for cancer therapy. Nat Rev Cancer. 2016; 16: 131-144.

31. Ni L, Lu J. Interferon gamma in cancer immunotherapy. Cancer Med. 2018; 7: 4509-4516.

32. Claus G, Konstantin K, Christos CZ, Katrin S, Sabine K, et al. Antitumor activities of interferon alpha, beta, and gamma and their combinations on human melanoma cells in vitro: changes of proliferation, melanin synthesis, and immunophenotype. The Journal of investigative dermatology. 1990; 6.

33. Belfield H, Chikh A, Ramadan S. Apoptosis methods and protocols. Cell Death and Differentiation. 2005; 12: 1361-1361.

34. Chen Y, Jiao B, Yao M, Shi X, Zheng Z, et al. IS G12 a inhibits HCV replication and potentiates the anti-HCV activity of IFN-alpha through activation of the Jak/STAT signaling pathway independent of autophagy and apoptosis. Virus Res. 2017; 227: 231-239.

35. Garcia-Diaz A, Shin DS, Moreno BH, Saco J, Escuin-Ordinas H, et al. Interferon Receptor Signaling Pathways Regulating PD-L1 and PD-L2 Expression. Cell Reports. 2017; 19, 1189-1201.

36. Zhang X, Bogunovic D, Payelle-Brogard B, Francois-Newton V, Speer SD, et al. Human intracellular ISG15 prevents interferon-alpha/beta over-amplification and auto- inflammation. Nature, 2015; 517: 89-93.

37. Ivashkiv LB, Donlin LT. a. Regulation of type I interferon responses. Nature Reviews Immunology. 2014; 14: 36-49.

38. Peng W, Liu C, Xu C, Lou Y, Chen J, et al. PD-1 blockade enhances T-cell migration to tumors by elevating IFN-gamma inducible chemokines. Cancer Res. 2012; 72: 5209-5218.

39. Dulos J, Carven GJ, Van Boxtel SJ, Evers S, Driessen-Engels, et al. PD-1 blockade augments Th1 and Th17 and suppresses Th2 responses in peripheral blood from patients with prostate and advanced melanoma cancer. J Immunother. 2012; 35: 169-178.

40. Greiner JW, Hand PH, Noguchi P, Fisher PB, Pestka S, et al. Enhanced expression of surface tumor-associated antigens on human breast and colon tumor cells after recombinant human leukocyte alpha-interferon treatment. Cancer Res.1984; 44: 3208-3214.

41. Gresser I, Maury C Brouty-Boye D. Mechanism of the antitumour effect of interferon in mice. Nature. 1972; 239: 167-168.

42. Hanahan D, Weinberg RA. Hallmarks of cancer: The next generation. Cell. 2011; 144: 646-674.

43. Martin M. Cutadapt Removes Adapter Sequences From High-Throughput Sequencing Reads. EMBnet Journal. 2011; 17: 10-12.